Methanol ice VUV photoprocessing: GC-MS analysis of volatile organic compounds

Ninette Abou Mrad, Fabrice Duvernay, Thierry Chiavassa, Grégoire Danger

Monthly Notices of the ROYAL ASTRONOMICAL SOCIETY

MNRAS **458,** 1234–1241 (2016) doi:10.1093/mnras/stw346
Advance Access publication 2016 February 15

Methanol ice VUV photoprocessing: GC-MS analysis of volatile organic compounds

Ninette Abou Mrad, Fabrice Duvernay, Thierry Chiavassa and Grégoire Danger*
Aix-Marseille Université, PIIM UMR-CNRS 7345, F-13397 Marseille, France

Accepted 2016 February 10. Received 2016 February 5; in original form 2015 December 9

ABSTRACT

Next to water, methanol is one of the most abundant molecules in astrophysical ices. A new experimental approach is presented here for the direct monitoring via gas chromatography coupled to mass spectrometry (GC-MS) of a sublimating photoprocessed pure methanol ice. Unprecedentedly, in a same analysis, compelling evidences for the formation of 33 volatile organic compounds are provided. The latter are C1–C6 products including alcohols, aldehydes, ketones, esters, ethers and carboxylic acids. Few C3 and all C4 detected compounds have been identified for the first time. Tentative detections of few C5 and C6 compounds are also presented. GC-MS allows for the first time the direct quantification of C2–C4 photoproducts and shows that their abundances decrease with the increase of their carbon chain length. These qualitative and quantitative measurements provide important complementary results to previous experiments, and present interesting similarities with observations of sources rich in methanol.

Key words: astrochemistry – molecular data – molecular processes – comets: general.

1 INTRODUCTION

Icy mantles surrounding dust grains in cold and dense molecular clouds are processed during the different phases accompanying the formation of low-mass stars and planetary systems (van Dishoeck & Blake 1998; Caselli & Ceccarelli 2012). Their original chemical composition mainly constituted of water (H_2O), ammonia (NH_3), methanol (CH_3OH), carbon monoxide (CO) and carbon dioxide (CO_2) (Gibb et al. 2000; Boogert et al. 2004; Dartois 2005; Zasowski et al. 2009; Boogert, Gerakines & Whittet 2015) evolves under radiations from surrounding stars. Such altered ices are furthermore thermo-processed during the formation of protostars, for instance, producing refractory organic residues after the sublimation of the most volatile compounds in the innermost parts of low- and high-mass protostellar envelopes (Ciesla & Sandford 2012). These regions known as hot cores and hot corinos are extensively observed using radio astronomy to identify their content in organic molecules (Requena-Torres et al. 2006; Requena-Torres et al. 2008; Herbst & van Dishoeck 2009). However, they are complex to be fully characterized due to plethora of observed rotational lines. This complexity is also observed in cometary gaseous environments, where similarity with interstellar ices is observed (Bockelée-Morvan et al. 2004; Mumma & Charnley 2011). To orient the search for new specific compounds in hot cores and in cometary environments, laboratory simulations have been developed, and consist in submitting ice analogues to various energetic processes to which astrophysical ices are subjected to (d'Hendecourt & Dartois 2001).

Among molecules of icy grains, methanol is in many cases and after water, one of the most abundant compounds and a source of reduced carbon. Some models present the methanol as a precursor of various complex organic molecules either in the gas phase or on dust grains. On grains, methanol photoproducts directly take a part in the formation of more complex molecules (Danger et al. 2012; Vinogradoff et al. 2012a) that form refractory compounds which stack on grains after water and volatile organic compounds (VOC) desorption (Danger et al. 2013). Consequently, increasing our knowledge of the methanol chemistry will give clues on molecules that could be detected in the gas phase of hot cores or cometary environments, as well as on the chemistry that may furthermore lead to the organic matter observed in meteorites, daughters of comets and asteroids. Several studies have reported the analysis of products in pure methanol or mixed methanol ices using infrared spectroscopy (Gerakines, Schutte & Ehrenfreund 1996), temperature programme desorption coupled to infrared analyses (Öberg et al. 2009), single photoionization reflectron time of flight mass spectrometry (MS) (Kaiser, Maity & Jones 2015; Maity, Kaiser & Jones 2015), or a two-step laser ablation and ionization MS (Henderson & Gudipati 2015). To date, from all these studies, up to 19 simple and complex photoproducts have been identified, and only few quantitative data were obtained on CH_3OH photodissociation yields (Gerakines et al. 1996; Öberg et al. 2009), which are primordial to estimate the detectability of methanol photoproducts in astrophysical environments.

* E-mail: gregoire.danger@univ-amu.fr

To expand the range of VOC identified after pure methanol ice processing and to allow their direct quantification, an analytical approach (VAHIIA system, standing for Volatile Analysis coming from the Heating of Interstellar Ice Analogues) based on gas chromatography (GC) coupled to MS has been developed (Abou Mrad et al. 2014). Considering the importance of methanol in astrophysical ices described earlier, we focus in this contribution on the use of the VAHIIA system for the identification and quantification of VOC formed after the Vacuum Ultra Violet (VUV) irradiation and the subsequent warming-up of a multilayered pure methanol ice. We also discuss the importance of the obtained results for the preparation of the analysis of more complex ice analogues as well as their potential benefits to astronomers and scientists searching for organic compounds in astrophysical environments.

2 METHODS

2.1 Experimental set-up and CH_3OH formation and photoprocessing

Experiments were carried out in an original set-up described previously (Abou Mrad et al. 2014). Briefly, methanol gases (for pesticide residue analysis, Fluka analytical from Sigma Aldrich) are deposited from a glass-line on a cold finger at 20 K inside a high vacuum chamber ($\sim 10^{-8}$ mbar). The finger is cooled using a closed-cycle helium refrigerator, and maintained using a 21 CTI cold head at 20 K during deposition and subsequent irradiation. The deposition of gas for ice formation can be monitored using a Bruker Tensor 27 Fourier transform infrared spectrometer. In order to increase the irradiation yield, the experiment was conducted as follows: a first ice of 6.84 μmol of methanol is deposited and irradiated for 24 h, then a second successive ice of 6.84 μmol of methanol is formed and irradiated for 24 h, and finally a third successive ice of 6.84 μmol of methanol is deposited and irradiated for 29 h. Irradiation is ensured by a UV light from a broadband hydrogen microwave-discharge lamp emitting 2.5 10^{13} photons cm^{-2} s^{-1} in the VUV range. Here, layers of each deposit are sufficiently thick to prohibit the UV irradiation of the previous photoprocessed ice. After irradiation, the vacuum chamber is warmed-up to 300 K with the cryogenic system switched-off, and all species sublimating from the ice are pumped and gradually preconcentrated during 16 h in the preconcentration loop of the VAHIIA interface directly connected to the vacuum chamber and to the GC-MS. A full description of this interface is reported elsewhere (Abou Mrad et al. 2014). Subsequently, the preconcentration loop is warmed and helium is added to reach a total pressure of 200 mbar which facilitates the sample transfer to the injection unit of the GC-MS. The experiment of CH_3OH photoprocessing is repeated three times to evaluate the uncertainty of GC-MS and infrared analysis.

Prior to the photochemistry experiment of methanol ice, a blank sample was run to discriminate potential contaminations occurring from the experimental set-up itself. It consisted of cooling the chamber to 20 K and irradiating the cold finger (with no sample on it) during 77 h (Supplementary Information, Fig. S1). A methanol blank was also conducted in the same conditions as the photochemistry experiment (quantity of methanol, temperature, duration. . .) but without irradiation to account for reactant contaminations. The same procedure described for the samples was applied for their analysis. Furthermore, a $^{13}CH_3OH$ (99 % atom ^{13}C from Sigma Aldrich) irradiation experiment was also performed under the same experimental conditions as for the $^{12}CH_3OH$ in order to verify that all photoproducts identified in this work come from methanol photoprocessing.

2.2 GC-MS conditions for sample analysis

The GC-MS used was purchased from Thermofisher (GC Trace 1310 and MS ion trap ITQ 900), and was modified in collaboration with Interscience Belgium for gaseous sample injection. The sample contained in the injection loop is transferred to the GC split/splitless injector, operated in split mode at 250 °C. The gaseous injection loop of the GC-MS (500 μL) is thermostated at 110 °C. A split ratio of 10 is used for the qualitative screening and quantification of photoproducts. The same experiment is conducted with a split ratio of 45 to quantify methanol after irradiation in order to avoid detector saturation. Analytes are separated on a Stabilwax-DA column purchased from Restek (Crossbond Carbowax Polyethylene glycol stationary phase, 30 × 0.25 mm i.d. × 0.50 μm). Helium is used as a carrier gas at a constant flow rate of 1 mL min^{-1}. Initial column temperature is of 45 °C for 3 min, followed by an increase of 5 °C min^{-1} to 70 °C held for 1 min, then of 15 °C min^{-1} until 220 °C with an isothermal hold of 2 min. The mass spectrometer transfer line is set to 250 °C. The ion source temperature is set to 250 °C and the maximum ion time in the trap is of 25 ms. The ion trap mass spectrometer is used in the electron impact ionization mode with an ionization energy of 70 eV. The signal is collected with a full scan mode in the mass range between 15 and 300 u and a scan event time of 0.16 s.

2.3 GC-MS peak identification process

The identification process of the sample chromatographic peaks lies in their comparison with a batch of analytical standards that might be present in the sample. Considering the possible VUV photochemistry induced in CH_3OH ice, 69 GC standards having up to six carbon atoms were selected. They include alcohols, aldehydes, ketones, acids, esters and ethers. All standards were introduced in the VAHIIA interface following the same procedure as for the irradiated samples. They have been preconcentrated directly in the preconcentration loop (Abou Mrad et al. 2014), either individually or in mixtures, and were analysed using the same GC-MS conditions as the sample, to determine their retention times on the chromatographic column, their specific mass spectra and their stability all along the analytical system. All standards are stable in our experimental conditions.

VOC were identified following a set of criteria to assign with acceptable uncertainty their presence in the sample. The first requires that the peak retention time should fall in the 95 % confidence interval of the replicated standard retention times ($n = 3$). When the peak retention time is very close to the limits of the 95 % confidence interval, a 99 % confidence interval is then accepted. In this case, compounds are not discarded at this stage of the identification process since other criteria are yet to be evaluated. The second criterion is the concordance between the fragmentation pattern of the mass spectrum of a sample peak and the corresponding standard (all mass fragments of a standard having a relative intensity lower than 10 % are neglected) (Supplementary Information, Fig. S3). This parameter is evaluated by a correlation coefficient R, and confirms the presence of compounds fitting with the previous retention time criterion if R values are beyond 0.75 (Table 1). In the case of co-eluting compounds, the mass spectrum of the sample peak is compared to a reconstructed spectrum where each of the co-eluting standard spectrum is added with a contribution optimized

Table 1. Volatile organic compounds identified from the photoprocessing of a pure methanol ice at 20 K and subsequently warmed up to 300 K. GC-MS quantification is also reported. Retention times of sample peaks (designated in Fig. 1) with standard error (sample R_t ±E, $n = 3$ for GC analysis) are reported, as well as the two other criteria used for peak identification in GC-MS: the correlation coefficient between mass spectra of the sample peak and expected standards (R), and the mass shift observed for a specific fragment between $^{12}CH_3OH$ and $^{13}CH_3OH$ experiments. Relative abundances are also reported (quantity of photoproducts/ CH_3OH consumed) with standard error (Relative abundance ± E, $n = 3$). IR corresponds to products identified only by infrared spectroscopy in this work. NIST corresponds to products identified in GC-MS by the comparison of their mass spectrum with the NIST database. Co (peak number) corresponds to co-eluting compounds. n.o. (not observed).

	Products identified	Molecular formula in Fig. 1)	Sample $R_t \pm E^b$ (peak position)	Standard $R_t \pm E^b$ (min)	R	$^{12}C/^{13}C$ experiments Fragment	$^{12}CH_3OH$ (Mw)	$^{13}CH_3OH$ (Mw)	Relative abundance $\pm E^b$ (%)
C0	water	H_2O	8.23 ± 0.06 (24)	8.26 ± 0.12[c]	0.9878	–	–	–	
C1	carbon monoxide	CO	IR						51 ± 3
	formaldehyde	H_2CO	IR						13 ± 1
	methanol	CH_4O	4.68 ± 0.07 (12)	4.58 ± 0.04	0.9729	$[CH_4O]^+$	32	33	
	carbon dioxyde	CO_2	1.65 (1)	–	NIST	$[CO_2]^+$	44	45	13 ± 3
	methane	CH_4	IR						20.2 ± 0.9
C2	acetaldehyde	C_2H_4O	2.35 ± 0.02 (3)	2.33 ± 0.02	0.9896	$[C_2H_4O]^{+\cdot}$	44	46	0.45 ± 0.02 [a]
	ethanol	C_2H_6O	5.40 ± 0.05 (17)	5.37 ± 0.05	0.9734	Co(17)			1.4 ± 0.6 [a]
	dimethyl ether	C_2H_6O	1.75 ± 0.01 (2)	–	NIST	$[C_2H_6O]^{+\cdot}$	46	48	
	acetic acid	$C_2H_4O_2$	15.34[e] (29)	15.33 ± 0.02	0.9819	$[C_2H_4O_2]^{+\cdot}$	60	n.o.	<0.17 [e]
	methyl formate	$C_2H_4O_2$	2.77 ± 0.03 (5)	2.74 ± 0.04	0.9926	$[C_2H_4O_2]^{+\cdot}$	60	62	0.19 ± 0.02
C3	propionaldehyde	C_3H_6O	3.07 ± 0.05 (6)	3.04 ± 0.04	0.8995	$[C_3H_6O]^{+\cdot}$	58	61	$6.3\ 10^{-3} \pm 2.2\ 10^{-3}$ [a]
	acetone	C_3H_6O	3.37 ± 0.04 (8)	3.34 ± 0.03	0.9983	$[C_3H_6O]^{+\cdot}$	58	61	$1.8\ 10^{-2} \pm 0.3\ 10^{-2}$ [a]
	propyl formate	$C_4H_8O_2$	5.22 ± 0.05 (16)	5.18 ± 0.04	[d]				
	2-propanol	C_3H_8O	5.22 ± 0.05 (16)	5.19 ± 0.05	0.9198	$[C_3H_7O]^{+\cdot}$	59	62	$5.5\ 10^{-2} \pm 2.9\ 10^{-2}$
	1-propanol	$C_3H_8O_2$	8.00 ± 0.06 (23)	7.97 ± 0.06	0.9719	$[C_3H_7O]^+$	59	62	$3.00\ 10^{-2} \pm 0.04\ 10^{-2}$
	methyl acetate	$C_3H_6O_2$	3.53 ± 0.04 (9)	3.51 ± 0.04	0.9996	$[C_3H_6O_2]^{+\cdot}$	74	77	$2.8\ 10^{-2} \pm 0.1\ 10^{-2}$
	dimethoxymethane	$C_3H_8O_2$	2.55 ± 0.03 (4)	2.53 ± 0.03	0.9944	$[C_3H_8O_2]^{+\cdot}$	76	79	$0.9\ 10^{-5} \pm 0.1\ 10^{-5}$
C4	butyraldehyde	C_4H_8O	4.29 ± 0.05 (10)	4.28 ± 0.04	0.9912	$[C_3H_7]^+$	43	46	$1.9\ 10^{-4} \pm 0.8\ 10^{-4}$
	isobutyraldehyde	C_4H_8O	3.28[e] (7)	3.30 ± 0.03	0.5983[d]	$[C_4H_8O]^{+\cdot}$	72	n.o.	
	2-butanone	C_4H_8O	4.75 ± 0.05 (13)	4.72 ± 0.06	0.9873	$[C_4H_8O]^{+\cdot}$	72	76	
	2-methyl-1-propanol	$C_4H_{10}O$	9.54 ± 0.07 (25)	9.52 ± 0.05[c]	0.9335	Co(25)			
	1-butanol	$C_4H_{10}O$	10.86 ± 0.04 (27)	10.80 ± 0.05	0.9752	$[C_4H_8]^{+\cdot}$	56	60	
	2-butanol	$C_4H_{10}O$	7.59 ± 0.06 (22)	7.56 ± 0.05	0.9758	$[C_3H_7O]^+$	59	62	
	ethyl acetate	$C_4H_8O_2$	4.46 ± 0.05 (11)	4.46 ± 0.06[c]	0.6634	$[C_2H_5O_2]^+$	61	63	
	methyl propionate	$C_4H_8O_2$	4.85 ± 0.05 (14)	4.84 ± 0.05	0.7601	$[C_4H_8O_2]^+$	88	92	$6.1\ 10^{-5} \pm 2.3\ 10^{-5}$
C5	pentanal	$C_5H_{10}O$	6.52 ± 0.05 (18)	6.55 ± 0.08[c]	0.9872	Co(18)			
	2-methyl butyraldehyde	$C_5H_{10}O$	4.94[e] (15)	4.99 ± 0.06	0.8876	$[C_5H_{10}O]^{+\cdot}$	86	91	
	Methyl isobutyrate	$C_5H_{10}O_2$	5.22 ± 0.05 (16)	5.18 ± 0.03	[d]				
	2-pentanone	$C_5H_{10}O$	6.52 ± 0.05 (18)	6.49 ± 0.06	0.9872	Co(18)			
	2-methyl-2-butanol	$C_5H_{12}O$	7.20 ± 0.06 (20)	7.19 ± 0.05	–0.361[d]	$[C_4H_9O]^+$	73	n.o.	
	2,2-dimethyl propanol	$C_5H_{12}O$	9.95 ± 0.05 (26)	9.94 ± 0.06	0.8535	$[C_4H_9]^+$	57	61	
	3-methyl-2-butanol	$C_5H_{12}O$	9.54 ± 0.07 (25)	9.51 ± 0.05[c]	0.9335	Co(25)			
	methyl butyrate	$C_5H_{10}O_2$	6.70 ± 0.05 (19)	6.68 ± 0.06	0.8008	$[C_4H_7O_2]^+$	87	91	
	2-methyl-1-butanol	$C_5H_{12}O$	12.04 ± 0.03 (28)	12.01 ± 0.01	0.8084	$[C_5H_{10}]^{+\cdot}$	70	n.o.	
C6	hexanal	$C_6H_{12}O$	9.54 ± 0.07 (25)	9.48 ± 0.06	0.9335	Co(25)			
	2-methyl pentanal	$C_6H_{12}O$	7.23 ± 0.06 (21)	7.21 ± 0.05[c]	0.8460	Co(21)			
	2,2-dimethyl butanal	$C_6H_{12}O$	5.40 ± 0.05 (17)	5.35 ± 0.03	0.9734	Co(17)			
	4-methyl-2-pentanone	$C_6H_{12}O$	7.23 ± 0.06 (21)	7.22 ± 0.07[c]	0.8460	Co(21)			

Notes. [a]Upper limit values since these compounds are expected to be co-eluting with other minor identified or unidentified compounds. [b]Error obtained with a 95 % confidence interval, except for [c](99 % of the confidence interval). [d]Peak samples fitting with retention time of standards but discarded due to low R values. [e]Upper value due to its low sensitivity and detection in only one of the replicate experiments.

to maximize the correlation coefficient R (Supplementary Information Fig. S4). The last criterion is based on the observation of photoproducts issued from the $^{13}CH_3OH$ experiment. Concretely, a characteristic fragment including carbon atoms is selected for each photoproduct of the $^{12}CH_3OH$ experiment (Table 1). A mass shift equal to the carbon number of this fragment is searched for in the $^{13}CH_3OH$ experiment. Its presence supports the confirmation of the compound identified and proves that it originates from $^{13}CH_3OH$. The molecular ion is privileged as the characteristic fragment if detected, independently of its abundance. Otherwise, the fragment is selected among the heaviest ones.

2.3 Quantification procedure of CH_3OH photoproducts

The VOC abundances are obtained relatively to the absolute quantity of photodissociated methanol (initial amount of methanol – remaining methanol). The absolute quantity of C2–C4 photoproducts was calculated using GC-MS calibration curves. A split ratio of 10 is used for the VOC quantification, and of 45 for quantifying the remaining methanol. Branching ratios require the knowledge of the initial amount of methanol deposited. However, the latter cannot be calculated with the GC-MS because it leads to detector saturation despite a split 45 used. A higher split ratio was not used

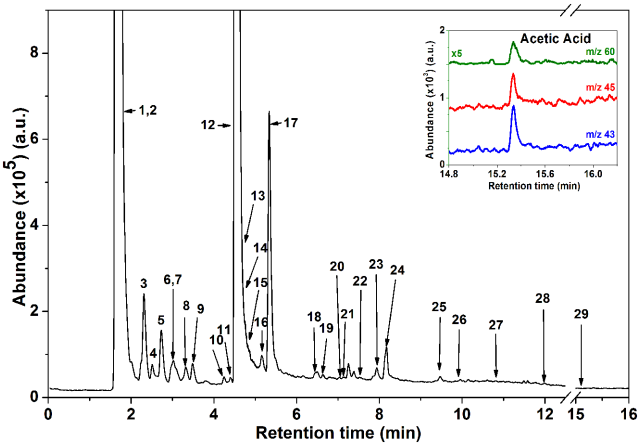

Figure 1 GC-MS chromatogram of the sublimated products of a photoprocessed CH_3OH ice as total ion current (TIC) from which the chromatogram of non-irradiated CH_3OH (blank CH_3OH) is subtracted (original chromatograms are presented in Supplementary Information, Fig. S1). All positive peaks are products formed during the methanol ice irradiation and its warming-up. Acetic acid (peak 29) is displayed as an example of an extracted ion chromatogram where m/z 43, 45 and 60 are recovered. Peaks 1 and 2 were identified according to the NIST database. Peaks 3–29 were investigated based on the comparison with standards and are reported in Table 1.

since it cannot be reproducible due to the experiment constraints. Therefore, the initial amount of methanol was obtained using the remaining amount of methanol after irradiation determined by GC-MS and the average remaining rate (ratio of remaining methanol to initial methanol) after 24 h obtained from infrared spectroscopy (58 ± 5 %). The latter was calculated from the methanol band area at 1025 cm^{-1} (A_x = 1.8 10^{-17} cm molecule^{-1}) in the infrared spectrum before and after irradiation. We deduce that 42 ± 5 % of the initial amount of methanol was irradiated. Relative abundances of C1 photoproducts (CO_2, CO, CH_4 and H_2CO) were calculated using infrared spectroscopy as the ratios of column density (N_x) of photoproducts relatively to the consumed CH_3OH column density (CH_4: 1304 cm^{-1}, A_x = 6.6 10^{-18} cm molecule^{-1}; CO: 2136 cm^{-1}, A_x = 1.1 10^{-17} cm molecule^{-1}; CO_2: 2341 cm^{-1}, A_x = 7.6 10^{-17} cm molecule^{-1}; CH_2O: 1494 cm^{-1}, A_x = 3.9 10^{-18} cm molecule^{-1}).

3 RESULTS

3.1 VOC identification

The GC-MS chromatogram of methanol photoprocessed ice from which the chromatogram of blank methanol is subtracted highlights the chemical diversity obtained after ice processing and warming. All positive peaks in Fig. 1 refer to compounds formed during the ice processing. A 'negative' peak is expected for methanol since it has been consumed during sample irradiation. However, a positive peak (12) is observed likely due to the saturation of the detector implying a non-linear response with the compound's quantity. The extraction of single ions from the total ion current (TIC) allows the detection of numerous peaks not perceptible in the TIC, strengthening the molecular diversity of the sample (Fig. 1 and Supplementary Information, Fig. S2). The identification of some of these peaks in the replicated experiment was based on three criteria (details in section Methods): retention time (sample R_t ± E versus standard R_t ± E in Table 1), correlation between mass fragmentation patterns of the sample and the standard (R in Table 1, Fig. 2), and mass shift in a $^{13}CH_3OH$ experiment (Table 1).

Among the chromatographic peaks detected, 29 have been selected considering our identification criteria (Peaks 1– 29 in Fig. 1, Table 1). 22 peaks have a retention time that matches only with one standard (examples in Fig. 2). The comparison of the mass fragmentation patterns of sample peaks and the expected standards reveals the presence of dimethoxymethane, methyl formate, acetone, methyl acetate, butyraldehyde, 2-butanone, 2-butanol, 1-propanol, 1-butanol, acetaldehyde and acetic acid (Table 1 for individual peak positions and structures in Fig. 3). Peaks 6, 11 and 19 are probably explained by propionaldehyde, ethyl acetate and methyl butyrate respectively, but the presence of other masses in the sample peaks compared to their corresponding standards suggests possible co-elution with unidentified compounds. Despite the similitude of standard and sample mass spectra, 2-methyl butyraldehyde, 2-2 dimethyl propanol and 2-methyl-1-butanol (the latter possibly co-eluting with unidentified compounds) are tentatively attributed due to the absence in the sample of low abundant masses present in the standards. Methyl propionate is also tentatively attributed since its expected chromatographic peak of mass 29 is masked by the highly abundant mass 29 of the remaining fraction of methanol (Supplementary Fig. S3). The attribution of all listed compounds is furthermore supported by the mass shift observed in the $^{13}CH_3OH$ experiment (Table 1). Even though no mass shift was observed for 2-methyl-1-butanol and acetic acid, their presence is not rejected since they were observed close to their detection limit in the $^{12}CH_3OH$ experiment. A small variability in their amounts may cause their non-detection in the ^{13}C labelled sample. Isobutyraldehyde and 2-methyl-2-butanol are expected (peaks 7 and 20, respectively) considering their retention time. However, the low-correlation coefficients ($R < 0.75$) and the absence of mass shift in the $^{13}CH_3OH$ experiment discard their presence. Peaks 1 and 2 are explained by carbon dioxide and dimethyl ether based on the presence of their main characteristic fragments [taken from the National Institute for Standards and Technology (NIST) database] and their mass shift in the $^{13}CH_3OH$ experiment. However, dimethyl ether cannot be confirmed by the retention time criterion due to the unavailability of the analytical standard.

The five remaining peaks (16, 17, 18, 21, 25) potentially correspond to a co-elution of several standards. Peak 17 can be explained by the simultaneous presence of ethanol and 2,2-dimethyl butanal, peak 18 by 2-pentanone and pentanal, peak 21 by 4-methyl-2-pentanone and 2-methyl-pentanal, and peak 25 by hexanal, 3-methyl-2-butanol and 2-methyl-1-propanol. Considering peak 16, the highest concordance in the mass spectra is obtained between the sample peak and 2-propanol only, discarding the presence from the sample of co-eluting methyl isobutyrate and propyl formate (Supplementary Information, Fig. S4). In addition to the 30 molecules above identified, 3 others have been also detected in the sample using their features in infrared spectroscopy: methane (1304 cm^{-1}), carbon monoxide (2139 cm^{-1}) and formaldehyde (1495 cm^{-1}) (Supplementary Information, Fig. S5). Our GC-MS system does not provide their separation and identification.

The VAHIIA system allows in only one analysis to determine 33 VOC of a pure irradiated methanol ice (Fig. 3). These photoproducts are constituted of 1 to 6 carbon atom compounds with various chemical functions, such as aldehydes (C2–C6), alcohols (C2–C5), ketones (C3–C6), esters (C2-C6), ethers (C3–C5) and carboxylic acids (C2). 12 attributed compounds in this work have already been identified with ambiguity for some of them in previous studies: methane, formaldehyde, acetaldehyde, ethanol, dimethylether,

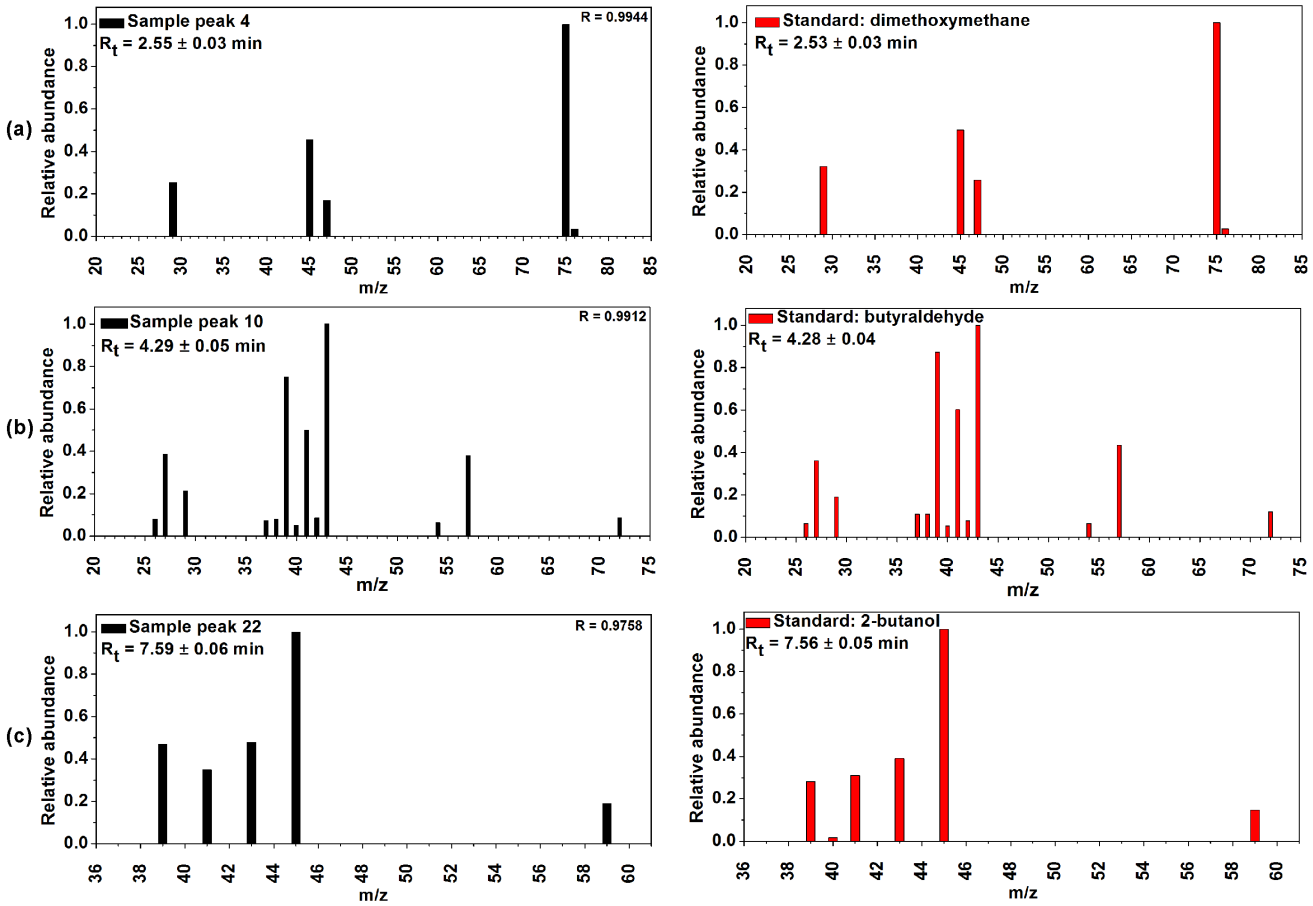

Figure 2. Examples of newly reported photoproducts identification based on the comparison of a sample peak mass spectrum (left spectra) and standard mass spectrum (right spectra) with corresponding retention time R_t. The correlation coefficients R between sample and standard spectra allow attributing sample peak 4 to dimethoxymethane (A), sample peak 10 to butyraldehyde (B) and sample peak 22 to 2-butanol (C).

acetic acid, methyl formate, propionaldehyde, acetone, 2-propanol, 1-propanol, methyl acetate. Even though some photoproducts are expected in the interstellar medium (ISM) and in comets as shown by previous laboratory experiments, they could not be detected currently in our experiments due to analytical set-up constraints. It is the case of formic acid, ethane, ketene, glycolaldehyde, 1,2-ethenediol, ethylene glycol, methoxymethanol and glycerol. In this study, 22 compounds have been identified for the first time with a majority having a carbon number higher than 3. Some of them corroborate assignments of C_3H_6O isomers (acetone, propionaldehyde), C_4H_8O isomers (butyraldehyde, butanone), $C_3H_6O_2$ isomers (methyl acetate), $C_4H_8O_2$ isomers (methyl propionate, ethyl acetate) and $C_4H_{10}O$ isomers (1-butanol and 2-butanol) suspected in CH_3OH-CO ices (Maity et al. 2015), highlighting once again the performance of the VAHIIA system to unveil the richness of photo-processed ice analogues. We note that among the 69 GC standards searched for, 39 were discarded for not fitting with our identification criteria or due to their low abundances (Table S2).

3.2 VOC quantification

In addition to the identification of CH_3OH photoproducts, a quantitative approach (details in Methods section) was conducted to obtain information on the abundance of photoproducts (C1, C2, C3 along with few C4) with respect to the consumed methanol (named relative abundance in Table 1). During our irradiation protocol, 42 ± 5 % of the initial amount of CH_3OH has been irradiated as determined by replicated infrared analysis. The highest abundances are obtained for C1 species, carbon monoxide being the most abundant (51 ± 3 %) followed by methane (20.2 ± 0.9 %), carbon dioxide (13 ± 3 %) and formaldehyde (13 ± 1 %). The relative abundance of all other photoproducts is below 3.0. An upper limit is given for acetic acid since it is close to its detection limit. Among these photoproducts, alcohols are the most abundant followed by aldehydes/ketones, esters and carboxylic acids. Dimethylether was not quantified due to unavailability of its standard. This evolution was already observed by Öberg et al. (Öberg et al. 2009) using infrared spectroscopy with also a higher abundance of ethanol relatively to acetaldehyde. In their experiment, dimethylether was present with a higher abundance than acetaldehyde.

Furthermore, our experiment shows that relative abundances of VOC decrease when their carbon chain is lengthened (Table 1). For instance, the ratio of aldehydes starts at 13 ± 1% for formaldehyde (C1) and decreases to 0.45 ± 0.02% for acetaldehyde (C2), 0.63 10^{-2} ± 0.22 10^{-2}% for propionaldehyde (C3) and 0.19 10^{-3} ± 0.08 10^{-3}% for butyraldehyde (C4). The same trend is observed for alcohols (Fig. 4). These observations are in total concordance with a non-oriented chemical synthesis that statistically decreases the abundance of compounds when their carbon number increases. This is particularly observed for the soluble organic matter of meteorites (Pizzarello, Cooper & Flynn 2006) and in comets for formaldehyde and acetaldehyde (Bockelée-Morvan et al. 2004). Furthermore, the

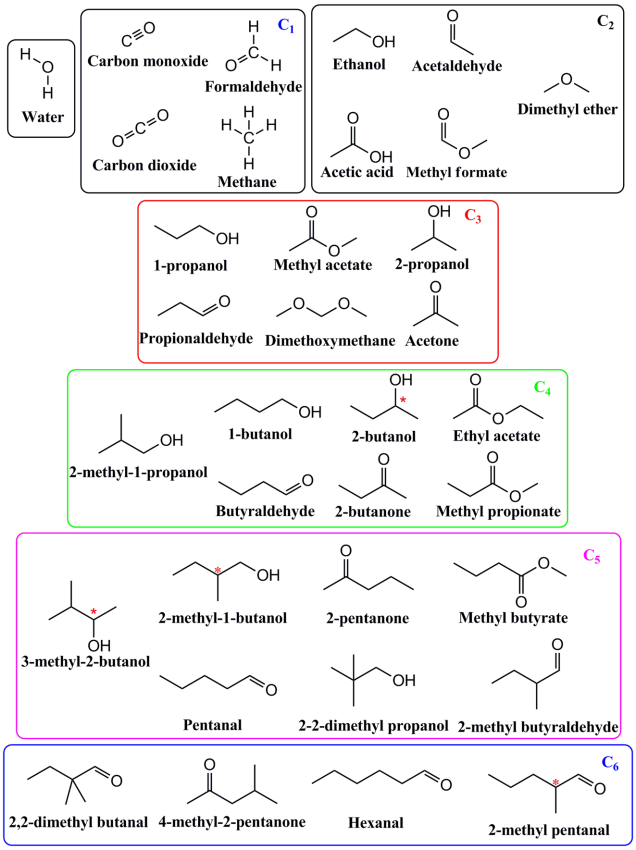

Figure 3. Structures of the 33 identified CH_3OH photoproducts in the current work. *asymmetric carbon.

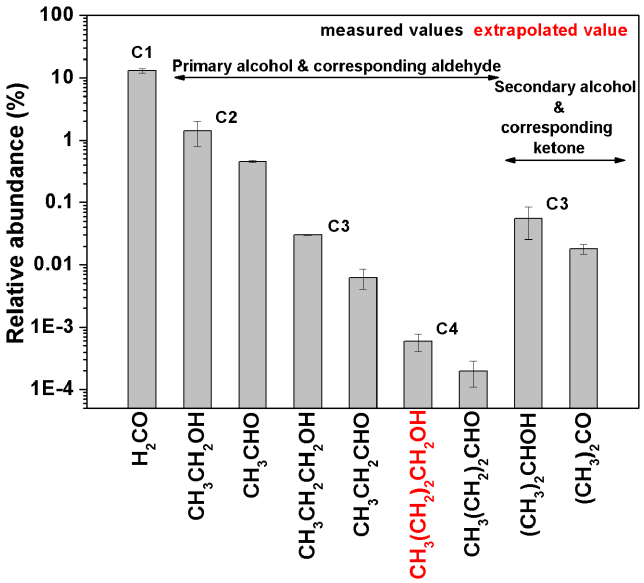

Figure 4. Relative abundances of alcohols and corresponding aldehydes or ketones produced from the photoprocessing of CH_3OH at 20 K. The error calculated from the replicate experiments ($n = 3$) is also represented.

comparison between aldehydes and alcohols shows that on average alcohol relative abundances are three times higher than their corresponding aldehydes, which is also observed for the secondary alcohol 2-propanol and acetone (Fig. 4). A connection could exist between these two family compounds, formation of aldehydes by alcohol photodegradation or alcohol formation from aldehyde hydrogenation. This ratio between alcohols and aldehydes having a same carbon number allows extrapolating from butyraldehyde the relative abundance of 1-butanol ($5.9\ 10^{-4}\ \% \pm 1.8\ 10^{-4}\%$), which is at a concentration lower than its limit of quantification (Fig. 4). Furthermore, relative abundances between primary (1-propanol) and secondary (2-propanol) alcohols are of the same order as well as their corresponding carbonyl derivatives.

4. DISCUSSION

The original qualitative and quantitative approaches presented in this contribution demonstrate that the molecular richness (several chemical functions, 19 atom compounds, chiral molecules) obtained by pure methanol ice VUV irradiation and heating is more diverse than suggested by previous studies (Gerakines et al. 1996; Henderson & Gudipati 2015; Maity et al. 2015; Öberg et al. 2009). The results obtained in the present study on the VUV photoprocessing of pure methanol ices are important for understanding the influence of other ice components on the chemical reactivity. In presence of other pristine molecules, a much more complex reactivity will indeed occur during the photoprocessing step. For instance, water has an active role in the reactivity of such ices. It acts as catalyst (Danger et al. 2014), allows a molecular trapping (Fresneau et al. 2014) and impacts the radical chemistry by modifying the relative abundances of photoproducts (i.e. hydroxyl and carboxylic acid compounds) (Oberg et al. 2009). On the other hand, ammonia will also form new photoproducts (i.e. amine, nitrile or amide derivatives) (Agarwal et al. 1985; Henderson & Gudipati 2015), as well as modify abundances of photoproducts characterized in this study. Furthermore, methanol photoproducts once formed can also thermally react during the heating step in presence of other photoproducts or pristine molecules. For instance, when an initial ice containing water, methanol and ammonia is irradiated and warmed-up, a complex residue is formed containing a huge diversity of molecules with masses up to 4.000 Da (Danger et al. 2013).

Among them, hexamethylenetetramine is one of the most abundant (Bernstein et al. 1995), and is proven to be formed from the reaction of ammonia with formaldehyde and formic acid (Vinogradoff et al. 2011, 2012b, 2013) which are both photoproducts of methanol. A similar case can occur for all other photoproducts (Vinogradoff et al. 2012a) which participate for a large part to the reactivity that leads to the molecular diversity observed (de Marcellus et al. 2015; Meinert et al. 2012). Experiments conducted on pure methanol ices are thus of prime interest to understand the complex chemical reactivity occurring in more representative ice analogues (mixtures of water, methanol and ammonia for instance). The variation of photoproducts relative abundances between pure methanol and complex ices will provide information on the reactivity induced by the addition of other components.

If methanol photoproducts are not fully consumed for residue formation, they can be released in the gas phase. 8 of the 33 identified compounds in this study have been detected in astrophysical environments, such as the ISM and circumstellar shells (Fig. 3): dimethyl ether (Requena-Torres et al. 2006), acetic acid (Remijan et al. 2002), ethanol (Requena-Torres et al. 2006), acetone (Snyder et al. 2002), propionaldehyde (Hollis et al. 2004), methyl acetate

(Tercero et al. 2013), acetaldehyde (Chengalur & Kanekar 2003) and methyl formate (Kobayashi et al. 2007). In the coma of comets Hale Bopp and Lovejoy, carbon monoxide, formaldehyde, methyl formate, acetaldehyde, ethanol and formic acid have been observed (Crovisier et al. 2004; Bockelee-Morvan et al. 2000; Biver et al. 2015). These two comets are rich in methanol. It is difficult to compare absolute quantity of compounds between observations and our experiments. However, the comparison of relative abundances between organic compounds is interesting. First, as for our experiments, alcohols are more abundant than their corresponding aldehydes (Biver et al. 2015). Furthermore, the ratio between ethanol and acetaldehyde is about 2.5 in both comets, a ratio similar to our experiments (ethanol/acetaldehyde = 3, 1-propanol/propionaldehyde = 3 and 2-propanol/acetone = 3). Even if a mechanistic investigation has to be performed to understand these similarities, these simple comparisons show that solid phase methanol photoprocessing could explain a part of molecules detected in the gas phase of objects rich in methanol.

Finally, the six CHO compounds detected by the Cometary Sampling and Composition Experiment (COSAC) mass spectrometer at the surface of the comet 67P/C-G (ethylene glycol, glycolaldehyde, acetaldehyde, propionaldehyde, acetone and 2-propanol) (Goesmann et al. 2015) have been identified in methanol ice experiments. Even if astrophysical ices are obviously more complex, experiments on pure methanol ices already confirm that a part of the detected compounds can be formed in the solid phase, and suggest a formation from the photoprocessing of methanol in the ice (Goesmann et al. 2015).

5. CONCLUSIONS

The direct analysis of sublimating methanol photoproducts using GC coupled to MS (GC-MS) highlights the chemical reactivity occurring in the solid phase and widens the list of compounds formed during the VUV processing of methanol ice in comparison to previous laboratory studies. 33 VOC (C1–C6) with various chemical functions, such as alcohol, aldehyde, ester, acid and ether, are expected to form in the solid phase of astrophysical ices as demonstrated in our experiment, and could be detected in the gas phase of hot regions. These results may be used by the scientific community to constraint models and interpret complex space mission data. Even though pure methanol ices are not totally representative of interstellar or cometary ones, this work allows for the first time the direct quantification of VOC sublimating from pure methanol ices, and it would be very interesting to monitor the evolution and the tendency of photoproducts abundances with those obtained in complex ices.

ACKNOWLEDGEMENTS

This work has been funded by the ANR project VAHIIA (Grant ANR-12-JS08-0001-01) of the French Agence Nationale de la Recherche and by the Foundation Aix-Marseille University for its post-doctoral funding 2015–2016. This work was furthermore supported by French national programmes, 'Programme National de Planétologie' (PNP, INSU), 'Programme de Physique et Chimie du Milieu Interstellaire' (PCMI, INSU) and the 'Centre National d'Etudes Spatiales' (CNES) from its exobiology program.

REFERENCES

Abou Mrad N., Duvernay F., Theulé P., Chiavassa T., Danger G, 2014, Anal. Chem., 86, 8391
Agarwal V. K. et al., 1985, Orig. Life Evol. Biosph., 16, 21
Bernstein D. I., Sandford S. A., Allamandola L. J., Chang S., Bernstein M., Scharberg M. A., 1995, ApJ, 454, 327
Biver N. et al., 2015, Sci. Adv., 1, e1500863
Bockelee-Morvan D. et al. 2000, A&A, 353, 1101
Bockelée-Morvan D., Crovisier J., Mumma M. J., Weaver H. A, 2004, in Festou M. C., Keller H. U., Weaver H. A., eds, Comets II. The Univ. Arizona Press, Tucson, AZ, p. 391
Boogert A. C. A., Gerakines P. A., Whittet D. C. B., 2015, ARA&A, 53, 541
Boogert A. C. A. et al., 2004, Astrophys. J. Suppl. Ser., 154, 359
Caselli P, Ceccarelli C., 2012, A&AR, 20, 56
Chengalur J. N., Kanekar N., 2003, A&A, 46, L43
Ciesla F. J., Sandford S. A., 2012, Science, 80, 1217291
Crovisier J., Bockelée-Morvan D., Colom P., Biver N., Despois D., Lis D. C., the Team for target-of-opportunity radio observations of comets, 2004, A&A, 418, 1141
d'Hendecourt L., Dartois E., 2001, Spectrochim. Acta. A., 57, 669
Danger G., Duvernay F., Theule P., Borget F., Chiavassa T., 2012, ApJ, 756, 11
Danger G. et al., 2013, Geochim. Cosmochim. Acta., 118, 184
Danger G. et al., 2014, Phys. Chem. Chem. Phys., 16, 3360
Dartois E., 2005, Space Sci. Rev., 119, 293
de Marcellus P., Meinert C., Myrgorodska I., Nahon L., Buhse T., d'Hendecourt Louis Le S., Meierhenrich U. J., 2015, Proc. Natl. Acad. Sci. USA, 112, 965
Fresneau A., Danger G., Rimola A., Theule P., Duvernay F., Chiavassa T., 2014, MNRAS, 443, 2991
Gerakines P. A., Schutte W. A., Ehrenfreund P., 1996, A&A, 312, 289
Gibb E., Nummelin A., Irvine W. M., Whittet D. C. B., Bergman P., 2000, ApJ, 545, 309
Goesmann F. et al., 2015, Science, 349, 6247
Henderson B. L., Gudipati M. S., 2015, ApJ, 800, 66
Herbst E., van Dishoeck E. F., 2009, ARA&A, 47, 427
Hollis J. M., Jewell P. R., Lovas F. J., Remijan A., Mollendal H., 2004, ApJ, 610, L21
Kaiser R. I., Maity S., Jones B. M., 2015, Angew. Chem., Int. Ed., 54, 195
Kobayashi K., Ogata K., Tsunekawa S., Takano S., 2007., ApJ, 657, L17
Maity S., Kaiser R. I., Jones B. M., 2015, Phys. Chem. Chem. Phys., 17, 3081
Meinert C., Filippi J.-J., de Marcellus P., Le Sergeant d'Hendecourt L., Meierhenrich U. J., 2012, Chempluschem., 77, 186
Mumma M. J., Charnley S. B., 2011, ARA&A, 49, 471
Öberg K. I., Garrod R. T., van Dishoeck E. F., Linnartz H., 2009, A&A, 913, 891
Pizzarello S., Cooper G. W., Flynn G. J., 2006, in Lauretta D. S., Mc Sween H. Y. Jr., eds, Meteorites and the Early Solar System II. The Univ. Arizona Press, Tucson, AZ, p. 625
Remijan A., Snyder L. E., Liu S.-Y., Mehringer D., Kuan, Y-J., 2002, ApJ, 576, 264
Requena-Torres M. A., Martín-Pintado J., Rodríguez-Franco A., Martín S., Rodríguez-Fernández N. J., de Vicente P., 2006, A&A, 455, 971
Requena-Torres M. A., Martin-Pintado J., Martin S., Morris M. R., 2008, ApJ, 672, 352
Snyder L. E., Lovas F. J., Mehringer D. M., Yanti Miao N., Kuan Y. J., Hollis J. M., Jewell P. R., 2002, ApJ, 578, 245
Tercero B., Kleiner I., Cernicharo J., Nguyen H. V. L., López A., Muñoz Caro G. M., 2013, ApJ, 770, L13
van Dishoeck E. F., Blake G. A., 1998, ARA&A, 36, 317
Vinogradoff V. et al., 2011, A&A, 530, A128
Vinogradoff V., Rimola A., Duvernay F., Danger G., Theule P., Chiavassa T., 2012b, Phys. Chem. Chem. Phys., 14, 12309
Vinogradoff V. et al., 2012a. J. Phys. Chem. A., 116, 2225
Vinogradoff V., Fray N., Duvernay F., Briani G., Danger G. et al., 2013, Astron. Astrophys., 551, A128
Zasowski G., Kemper F., Watson D. M., Furlan E., Bohac C. J.,, Hull C., Green J. D., 2009, ApJ, 694, 459

SUPPORTING INFORMATION

Additional Supporting Information may be found in the online version of this article:

Figure S1. GC-MS chromatograms of the $^{12}CH_3OH$ irradiated sample, the $^{13}CH_3OH$ irradiated sample, the $^{12}CH_3OH$ non-irradiated sample and the vacuum chamber blank.
Figure S2. Examples of extracted ion chromatograms (m/z 57 and m/z 39) of the CH_3OH photoprocessed sample. * represents attributed peaks.
Figure S3. Comparison of sample peak spectrum and standard spectrum for individual compounds. R represents the correlation coefficient between the sample and expected standard. The peak numbers correspond to Fig. 1.
Figure S4. Comparison of sample peak spectrum and reconstructed standard spectrum for co-eluting compounds. R represents the correlation coefficient between the sample and expected standards. The peak numbers correspond to Fig. 1.
Figure S5. Infrared spectrum of CH_3OH before and 24 h after irradiation.
Table S1. Compounds searched for but not detected in our study.
(http://www.mnras.oxfordjournals.org/lookup/suppl/doi:10.1093/mnras/stw346/-/DC1).

Please note: Oxford University Press is not responsible for the content or functionality of any supporting materials supplied by the authors. Any queries (other than missing material) should be directed to the corresponding author for the article.

This paper has been typeset from a TEX/LATEX file prepared by the author.